Journal of Orthopaedic Translation 48 (2024) 146–155

Contents lists available at ScienceDirect

Journal of Orthopaedic Translation

journal homepage: www.journals.elsevier.com/journal-of-orthopaedic-translation

Original Article

Strontium zinc silicate simultaneously alleviates osteoporosis and sarcopenia in tail-suspended rats via Piezo1-mediated Ca^{2+} signaling

Lingwei Huang [a,b,c,1], Yiren Jiao [a,b,1], Hangbin Xia [a,b,d], Huili Li [a,b,d], Jing Yu [a,b], Yumei Que [a,b], Zhen Zeng [a,b,c], Chen Fan [a,b], Chen Wang [b], Chen Yang [a,b,**], Jiang Chang [a,b,e,*]

[a] Joint Centre of Translational Medicine, The First Affiliated Hospital of Wenzhou Medical University, Wenzhou, 325000, China
[b] Zhejiang Engineering Research Center for Tissue Repair Materials, Wenzhou Institute, University of Chinese Academy of Sciences, Wenzhou, 325000, China
[c] College of Materials Science and Opto-electronic Technology, University of Chinese Academy of Sciences, Beijing, 100049, China
[d] School of Ophthalmology and Optometry, School of Biomedical Engineering, Wenzhou Medical University, Wenzhou, 325027, China
[e] Shanghai Institute of Ceramics, Chinese Academy of Sciences, Shanghai, 200050, China

ARTICLE INFO

Keywords:
Intracellular Ca^{2+}
Myogenesis
Osteogenesis
Osteosarcopenia
Piezo1
Strontium zinc silicate

ABSTRACT

Background: Long-term physical inactivity probably leads to a co-existence of osteoporosis and sarcopenia which result in a high risk of falls, fractures, disability and even mortality. However, universally applicable and feasible approaches are lacking in the concurrent treatment of osteoporosis and sarcopenia. In this study, we evaluated the effect of strontium zinc silicate bioceramic (SZS) extract on osteoporosis and sarcopenia and explored its underlying mechanisms.

Methods: Hindlimb osteoporosis and sarcopenia were established in a tail-suspended rat model. The bones were conducted μCT scanning, histological examination, and gene expression analysis, and the muscles were conducted histological examination and gene expression analysis. *In vitro,* the effect of SZS extract on osteoblasts was determined by alizarin red S staining, immunofluorescence and qPCR. Similarly, the effect of SZS extract on myoblasts was determined by immunofluorescence and qPCR.. At last, the role of Piezo1 and the change of intracellular calcium ion (Ca^{2+}) were explored through blockading the Piezo1 by GsMTx4 in MC3T3-E1 and C2C12 cells, respectively.

Results: We found that SZS extract could concurrently and efficiently prevent bone structure deterioration, muscle atrophy and fibrosis in hind limbs of the tail-suspended rats. The *in vivo* study also showed that SZS extract could upregulate the mRNA expression of Piezo1, thereby maintaining the homeostasis of bones and muscles. *In vitro* study demonstrated that SZS extract could promote the proliferation and differentiation of MC3T3-E1 and C2C12 cells by increasing the intracellular Ca^{2+} in a Piezo1-dependent manner.

Conclusion: This study demonstrated that SZS extract could increase Piezo1-mediated intracellular Ca^{2+}, and facilitate osteogenic differentiation of osteoblast and myogenic differentiation of myoblasts, contributing to alleviation of osteoporosis and sarcopenia in a tail-suspended rat model.

The translational potential of this article: The current study might provide a universally applicable and efficient strategy to treat musculoskeletal disorders based on bioactive ceramics. The verification of the role of Piezo1-modulated intracellular Ca^{2+} during osteogenesis and myogenesis provided a possible therapeutic target against mechanical related diseases.

1. Introduction

Long-term physical inactivity such as spaceflight, bedrest or spinal cord injury usually leads to osteoporosis and sarcopenia [1–3]. The coexistence of osteoporosis and sarcopenia usually results in more adverse outcomes than when either condition occurs independently, leading to a higher risk of falls, fractures, disability, and even mortality [2]. To counteract the disuse-induced bone loss and muscle atrophy

* Corresponding author. Joint Centre of Translational Medicine, the First Affiliated Hospital of Wenzhou Medical University, Wenzhou, 325000, China.
** Corresponding author. Joint Centre of Translational Medicine, the First Affiliated Hospital of Wenzhou Medical University, Wenzhou, 325000, China.
E-mail addresses: cryangchen@ucas.ac.cn (C. Yang), jchang@mail.sic.ac.cn (J. Chang).
[1] Lingwei Huang and Yiren Jiao contributed equally to this work.

https://doi.org/10.1016/j.jot.2024.07.014
Received 24 April 2024; Received in revised form 30 July 2024; Accepted 31 July 2024

simultaneously, physical exercises emerge as the predominant clinical strategy with well-established therapeutic efficacy [4]. However, physical exercise is challenging for patients with mobility issues, and thus, it is imperative to develop alternative therapeutic approaches to target osteoporosis and sarcopenia simultaneously.

Modeling the biological process through which exercise therapy operates might lead to therapeutic effects akin to those achieved through physical activity. The core of exercise therapy is to provide mechanical stimulation, which plays a crucial role in the maintenance of bone and muscle homeostasis [5,6]. The adaptation of bones and muscles to their mechanical environment vigorously relies on mechanosensors including Piezo channel, two-pore potassium (K2P) channel, hyperosmolality-gated Ca-permeable (OSCA/TMEM63) channel and transient receptor potential (TRP) channel [7,8]. Among these ion channels, Piezo1 is inherently mechanosensitive and exhibits high sensitivity than the other ion channels which attracts increasing interest [8]. Upon mechanical stimuli, Piezo1 is activated with enhanced calcium ion (Ca^{2+}) influx, which promotes the phosphorylation and activation of protein kinase B (Akt), stimulating osteogenic differentiation of bone marrow mesenchymal stem cells and the protein synthesis in skeletal muscle cells, conducing to the formation of both bones and skeletal muscles [9–11]. Wang et al. and Li et al. have proved that mechanical stimuli activates Piezo1 and further improves the proliferation/differentiation of osteoblasts and osteogenic gene and protein expression by osteocytes, ultimately contributing to bone formation and the enhancement of bone strength [12,13]. Not limited to the bones, Piezo1 is also involved in the process during which mechanical loading prevents the activation and p53-mediated senescence of muscle stem cells [14]. Mechanical unloading induces the downregulation of Piezo1 which reduces cytosolic Ca^{2+} concentration and induces Krüppel-like factor 15 and interleukin 6 (IL-6) expression in skeletal muscles, contributing to muscle atrophy [15]. Therefore, it is reasonable to hypothesize that Piezo1 serves as a pivotal regulator of bone and muscle tissue regeneration and activation of Piezo1 may be beneficial in simultaneously attenuating bone loss and muscle atrophy.

Direct stimulation of Piezo1 *via* ion manipulation emerges as a readily accessible strategy, given the mechanosensitive nature of Piezo1 as an ion channel protein. Though chemical compounds Yoda1, Jedi1 and Jedi2 are proposed as Piezo1 agonists to promote osteogenesis and myogenesis, they have limitations such as drug resistence, unknown biosafety, pricey, and relatively low aqueous solubility and potency [7]. Inorganic ions are promising to promote tissue regeneration due to their low drug resistence, cheapness, good biocompatibility and versatility. Divalent ions such as strontium ion (Sr^{2+}) and magnesium ion (Mg^{2+}) are also able to promote Ca^{2+} influx in cardiac myocytes [16], indicating the potential ability of Sr^{2+} and Mg^{2+} to activate the Ca^{2+}-associated ion channel Piezo1. Another study also shows that replacing the Mg^{2+} with Zn^{2+} increases approximately 100-fold Piezo1 currents in human embryonic kidney cells [17], implying a higher ability of Zn^{2+} in promoting the Piezo1-mediated Ca^{2+} influx than Mg^{2+}. Other than Sr^{2+} and Zn^{2+}, silicate ions (SiO_3^{2-}) also exhibit their role in regulating intracellular Ca^{2+}. A study reports that oral administration of SiO_3^{2-} promotes the mineral metabolism of calcium and magnesium in rats [18]. The extract of calcium silicate cement containing 4 mM SiO_3^{2-} significantly promotes the formation of calcium matrix by osteoblast-like cells [19]. Moreover, after pre-incubation with a bioactive glass containing 60 % of silicon, the intracellular Ca^{2+} signals increase sharply in osteoblasts [20]. These findings allude that SiO_3^{2-} is probably also involved in the Piezo1-mediated Ca^{2+} influx. However, the effect of Sr^{2+} and Zn^{2+} on the Ca^{2+} influx in both osteoblasts and myoblasts, and the effect of SiO_3^{2-} on the Ca^{2+} influx in myoblasts have yet to be elucidated. Our prior investigations have provided evidence that the amalgamation of Sr^{2+}, Zn^{2+}, and SiO_3^{2-} yields more potent biological functionalities than their individual counterparts, and the synthetic Sr-Zn-Si bioceramic ($Sr_2ZnSi_2O_7$, SZS) emerges as a promising candidate for the simultaneous sustained release of Sr^{2+}, Zn^{2+}, and SiO_3^{2-} ions [21–23]. Inspired by these findings, we hypothesized that the utilization of a combination of ions (Sr^{2+}, Zn^{2+}, and SiO_3^{2-}) derived from the Sr-Zn-Si bioceramic could potentially emulate the impact of mechanical loading in activating Piezo1 and its ensuing Ca^{2+} influx to mitigate disuse-induced bone loss and muscle atrophy.

To verify this hypothesis, we synthesized SZS and verified the effect of its extract on the prohibition of osteoporosis and sarcopenia in a tail-suspension rat model. Furthermore, we explored the effect of the SZS extract on mechanosensor Piezo1 and its downstream targets both *in vivo* and *in vitro* by utilizing osteoblasts and myoblasts. The current study may provide a universally applicable and efficient strategy to treat musculoskeletal disorders based on bioactive ceramics.

2. Materials and methods

2.1. Preparation of SZS extract

SZS powders were synthesized in a sol–gel method as we previously reported [24]. The phase and morphology of the synthetic powders were characterized using a X-ray diffractometer (D8 ADVANCE, Bruker, Germany) and a scanning electron microscope coupled with energy dispersive spectroscopy (SEM-EDS, Phenom Pharos, Phenom, Netherlands). For SZS extract preparation, the SZS powders were soaked into saline, α-minimum essential medium (α-MEM, Gibco, China) or Dulbecco's modified Eagle medium (DMEM, Yeasen, China) with a ratio of 200 mg/mL at 37 °C for 24 h, respectively. These mixtures were centrifuged at 4500 rpm for 10 min using a high-speed desktop refrigerated centrifuge (H1850R, cence®, China), and their supernatants were sterilized with a 0.22-μm Millipore filter (Millex®-GP, Merck Millipore, Ireland), respectively.

The saline extract of SZS was used for animal administration. The α-MEM and DMEM extracts of SZS were gradiently diluted to a concentration of 1/2, 1/8, 1/32, 1/128 and 1/512 of the original concentration. After adding with 10 % fetal bovine serum (FBS, ExCell Bio, China), 100 unit/ml penicillin and 100 μg/mL streptomycin (Yeasen, China), the diluted SZS extracts were utilized to culture osteoblasts (MC3T3-E1, Chinese Academy of Sciences, China) and myoblasts (C2C12, Chinese Academy of Sciences, China), respectively.

2.2. Establishment of tail-suspended rats and administration of SZS extract

Eighteen nine-week-old male Sprague–Dawley rats were purchased from the Zhejiang Provincial Laboratory Animal Center. All the procedures of the whole experiments were under the guidelines of the Animal Research and Ethics Committee of the Wenzhou Institute of the University of Chinese Academy of Sciences, and were approved by the Animal Research and Ethics Committee of Wenzhou Institute of University of Chinese (WIUCAS22122601). After five days' acclimation, the animals were randomly divided into three groups, including age-matched control (CNTL, $N = 6$) group, hindlimb unloading (HU, $N = 6$) group, HU with SZS treatment (HU + SZS, $N = 6$) group. All rats were singly housed and were provided with food and water ad libitum. The HU rats were tail-suspended from the onset of the experiment as described in a previously published work [25]. Briefly, the tail of a rat was cleaned with 75 % alcohol and shaved, which was followed by benzoin tincture smearing for adherence to a medical tape. Then, the medical tap was hitched to suspend the rat's hind limbs while allowing the rat to move freely in the cage with a 30° head-down tilt. The rats in the CNTL group and the HU group were administrated saline, and the rats in the HU + SZS group were administrated saline extracts of SZS intravenously, respectively. The intravenous administration was performed every other day and orderly in a dose of 1 mL/rat/time for two weeks.

2.3. Muscle strength and mass measurement

At the end of the experiment, all rats were weighed and their hindlimb grip force was measured. The muscle strength of rat hind limbs was assessed using a grip strength meter (LJ800-012, Nscing Es, China) following a previously published protocol [26]. Briefly, relax a rat before the testing, and then put the two hind paws of the rat onto a grip rod and pull the tail slowly to record the peak force. Then, animals were sacrificed to collect femurs, tibias, as well as tibialis anterior (TA), extensor digitorum longus (EDL), fibularis longus (FL), gastrocnemius (GA) and soleus (SOL) muscles. The fresh mass of the collected muscles was measured, and the relative muscle mass was calculated by muscle mass/body weight × 100 %.

2.4. μCT analysis of proximal tibias and distal femurs

For μCT analysis, proximal tibias and distal femurs were performed μCT scanning using a desktop device (Skyscan1276, Bruker, Germany) with a voltage of 100 kV and a current of 200 μA. Projection images with an isotropic pixel size of 18 μm were acquired for reconstruction and segmentation of trabecular bone within approximately 5 mm underlying articular cartilage using analysis software (CTAn, Bruker, Germany). The bone volume fraction (bone volume/tissue volume, BV/TV), trabecular thickness (Tb.Th), trabecular number (Tb.N), trabecular separation (Tb.Sp) and bone mineral density (BMD) of the segmented trabecular bone were analyzed.

2.5. Histological analysis and qPCR analysis

All the bone and muscle samples from hind limbs were fixed with 4 % paraformaldehyde, and bone samples were decalcified in ethylenediaminetetraacetic acid (EDTA) solution. Then, the bone and muscle samples were embedded in paraffin for histological analysis. 5-μm-thick bone sections were prepared for Masson's trichrome staining using the Masson's Trichrome Stain Kit (Solarbio, China) to assess the newly formed bone and mature bone ratio and the deposition of collagens in muscles. Hematoxylin and eosin (H&E, Beyotime, China) staining was conducted to analyze the mean value and relative distribution of the cross-sectional area (CSA) of muscle fibers.

The gene expression of Piezo1, runt-related transcription factor 2 (Runx2) and alpha-1 type I collagen (Col1α1) in tibias, as well as the gene expression of Piezo1, myomaker (Mymk) and myogenin (Myog) in GA and SOL muscles were identified by qPCR analysis. Briefly, tissue RNA was isolated from tissues using RNAiso Plus (Takara, Japan) according to the manufacturer's instructions. Then, the collected RNA samples were purified and reverse transcribed to single-strand cDNA using a HiScript II Q RT SuperMix for qPCR (+gDNA wiper) Synthesis Kit (Vazyme, China). The gene expression was detected using ChamQ SYBR qPCR Master Mix Kit (Vazyme, China) for a one-step real-time quantitative polymerase chain reaction according to the manufacturer's instruction using a LightCycler® 480 system (Roche, USA). The primer sequences of genes glyceraldehyde 3-phosphate dehydrogenase (Gapdh), Piezo1, Runx2, Col1α1, Myog and Mymk are listed in Table S1. The relative quantification in mRNA expression was performed using the $2^{-\Delta\Delta Ct}$ method [27]. All the fold changes in target gene expression (*i.e.* gene expression levels) were normalized to Gapdh.

2.6. Cell experiments

2.6.1. Effect of SZS extract on cell viability

MC3T3-E1 and C2C12 cells were seed into 96-well culture plates with a density of 1×10^3 cells/well, and cultured in growth medium supplemented with varying concentrations of SZS extract. The culture medium was changed every other day. After cultured for three or five days, the cell activity (indicated by OD value) was detected with the Cell Counting Kit-8 (CCK-8, Yeasen, China) according to the manufacturer's instruction using a microplate reader (EPOCH2NS, BioTek instruments, USA). The concentration of SZS extracts that exhibited optimal cell activity of MC3T3-E1 and C2C12 cells was selected to examine the effect of the SZS extract on osteogenesis and myogenesis *in vitro*, respectively.

2.6.2. Effect of SZS extract on osteogenesis of MC3T3-E1 cells

To evaluate the effect of SZS extract on osteogenesis, we analyzed the formation of bone nodules and the biochemical changes of osteoblasts. MC3T3-E1 cells were cultured in a 6-well culture plate with osteogenic differentiation medium containing 50 μg/mL ascorbic acid (Sinopharm Chemical Reagent, China), 10 mM β-glycerophosphate disodium (Macklin, China) and 10 nM dexamethasone (Macklin, China) without (CNTL group) or with the SZS extract (SZS group). The culture medium was changed every other day. After one-week culture, the cells was either stained with alizarin red S staining kit (Beyotime, China) to quantify mineralized bone nodules or for gene expression analysis of Piezo1, Runx2 and Col1α1.

2.6.3. Effect of SZS extract on myogenesis of C2C12 cells

To assess the effect of SZS extract on myogenesis, we analyzed the formation of myotubes and the biochemical changes of myoblasts. For immunofluorescence staining of myotubes, C2C12 cells were seeded in a 24-well plate and cultured in differentiation medium (high-glucose DMEM with 2 % horse serum (Cytiva, USA) and 1 % penicillin-streptomycin) with (SZS group) or without SZS (CNTL group). The culture medium was changed every other day. After culturing for five days, the cells were fixed, permeabilized and blocked. Then, the cells were stained with a primary anti-body Anti-Myosin (Boster, China) at 4 °C overnight, followed by incubation with secondary antibody Cy3-conjugated Affinipure Goat anti-Mouse IgG(H + L) (Proteintech, USA) and nuclei staining with DAPI in the dark. The stained cells were visualized using a fluorescence microscope (Axio Vert.A1, ZEISS, Germany), and the nuclei number per myotube and the fusion index (nuclei number inside myotube/total nuclei number × 100 %) were analyzed using the ImageJ software (ImageJ 1.45s, National Institutes of Health, USA). For biochemical analysis, C2C12 cells were cultured in a 6-well plate in differentiation medium with or without SZS extract for five days. The culture medium was changed every other day. The relative gene expression of Piezo1, Myog and Mymk were analyzed.

2.6.4. Effect of SZS extract on the Piezo1-mediated signaling

MC3T3-E1 and C2C12 cells were seeded into a 6-well plate and cultured in the presence or absence of SZS extract with or without 0.5 μM Piezo1 blocker grammostola spatulata mechanotoxin 4 (GsMTx4) (MedChemExpress, USA) for 48 h, and the relative mRNA expression of Piezo1 was analyzed, respectively. To further explore whether SZS extract promote osteogenesis and myogenesis *via* the Piezo1-mediated Ca^{2+} signaling, we utilized GsMTx4 to examine the roles of Piezo1 in osteoblast-mediated bone formation and myoblast-modulated muscle formation after SZS treatment. Inspired by the knowledge that Piezo1 activation increases intracellular Ca^{2+} which activates Akt [28], we detected the intracellular Ca^{2+} of osteoblasts and myoblasts for the evaluation of the Piezo1 activation. To perform this, MC3T3-E1 cells and C2C12 cells were seeded into a 24-well plate with a density of 2×10^4 cells/well, respectively. The cells were cultured for 48 h in the absence or presence of SZS extract with or without 0.5 μM GsMTx4, respectively. The cells were loaded with 5 μM Fluo-4 (Solarbio, China) and incubated at 37 °C for 20 min, which was followed by another incubation with HBSS solution for 40 min (Solarbio, China). After washing with HEPES buffer, the fluorescence images were collected using a fluorescence microscope (Axio Vert.A1, ZEISS, Germany), and the mean fluorescence intensity of Ca from each image was quantified using the ImageJ software (ImageJ 1.45s, National Institutes of Health, USA).

2.7. Statistical analysis

Statistical analyses were conducted using a Prism software (Version 5.01, GraphPad, USA). All data were presented as mean with the standard error of the mean (SEM), and P values were determined by an unpaired two-tailed Student's t-test or one-way analysis of variance (ANOVA) with the Fisher's least significant difference (LSD) test. The significance levels for all the tests were $0.01 \leq {}^{*}P < 0.05$, $0.001 \leq {}^{**}P < 0.01$ and ${}^{***}P < 0.001$, and $P > 0.05$ was indicated by NS (not significant).

3. Results

3.1. Characterization of SZS powders and extract

The XRD patterns confirmed that the purity of the synthesized SZS powders (Fig. S1A). The SEM with energy dispersive spectroscopy (EDS) further confirmed that the components O, Sr, Si and Zn were with atomic percentages of 54.65 %, 19.02 %, 16.72 % and 9.61 %, which was close to the atomic ratio in SZS (Figs. S1B–D).

3.2. SZS extract allivates the decrease of hindlimb grip force in HU rats

The hindlimb unloading rat model was established through tail suspension. Simultaneously, SZS extract was injected intravenously to investigate its impact on the bone and muscle of HU rats (Fig. 1A). The results demonstrated that two weeks' HU significantly decreased the body weight of rats, when compared to the CNTL rats (Fig. 1B). However, in the aspect of hindlimb grip force, compared to the CNTL group, HU significantly reduced (decreased by 42.41 %) the hindlimb grip force of rats, which was almost completely recovered to the level of the CNTL group after SZS treatment (Fig. 1C). Thus, administration of SZS extract showed potential for reversing muscle strength loss in HU rats.

3.3. SZS extract alleviates HU-induced bone loss

To assess the effect of SZS extract on HU-induced bone loss, μCT analysis and histological analysis were performed. μCT analysis revealed a significant degradation of the trabecular microstructure in both proximal tibias and distal femurs after HU, which was reversed by SZS extract (Fig. 2A; Fig. S2A). Specifically, compared to the CNTL group, HU led to lower trabecular bone volume fraction (BV/TV, Fig. 2B; Fig. S2B), thinner trabeculae (Tb.Th, Fig. 2C; Fig. S2C), smaller trabecular number (Fig. 2D), larger trabecular separation (Tb.Sp, Fig. 2E; Fig. S2E), as well as lower bone mineral density (BMD, Fig. 2F; Fig. S2F) in the proximal tibias and distal femurs, respectively. SZS administration significantly restored the all above indicators except for the trabecular BMD in distal femurs (Fig. 2; Fig. S2). There were no significant difference in the trabecular number in the distal femurs between the HU and CNTL groups, as well as between the HU and HU + SZS groups (Fig. S2D). Furthermore, Masson's trichrome staining results showed that HU reduced the accumulation of collagens in the proximal tibias when compared to the CNTL group, and SZS treatment significantly increased the collagen formation in the proximal tibias of HU rats (Fig. 2G and **H**). Collectively, SZS extract probably prohibited the HU-induced deterioration of bone microstructure in rats.

3.4. SZS extract alleviates HU-induced muscle atrophy

To investigate the effect of SZS extract on HU-induced muscle atrophy, the relative mass and histological morphology of skeletal muscles were assessed in the HU rat model. The morphological diagram showed that the volume of GA, SOL, TA, EDL and FL muscles was smaller in the HU group than in the CNTL group, while the volume of these muscles was larger in the SZS group than in the HU group (Fig. 3A; Fig. S3A). Specifically, HU led to a significant reduction of the relative mass of GA (decreased by 24.31 %), SOL (decreased by 54.97 %), TA (decreased by 15.88 %), EDL (decreased by 5.80 %) and FL (decreased by 26.43 %) muscles (Fig. 3B and **C**; Figs. S3B–D). After being treated with SZS extract, the relative mass of GA, SOL, TA, EDL and FL muscles became larger in the HU + SZS group than the HU group and restored to 82.90 %, 74.25 %, 92.94 %, 100.44 % and 88.44 % of the CNTL group, respectively (Fig. 3B and **C**; Figs. S3B–D). Then, GA and SOL muscles were selected to perform further histological analysis and gene expression analysis. H&E staining results showed that HU caused considerable atrophy of the mean CSA of GA (decreased by 41.33 %) and SOL (decreased by 84.43 %) muscle fibers, compared to the CNTL group (Fig. 3D–F). SZS treatment significantly increased the mean muscle fiber CSA of the GA rather than SOL muscles in the HU rats, and the mean muscle fiber CSA of the GA and SOL muscles was recovered to 84.76 % and 16.95 % of the CNTL group, respectively. Specifically, a higher relative distribution of CSA <1500 μm^2 and a lower relative distribution

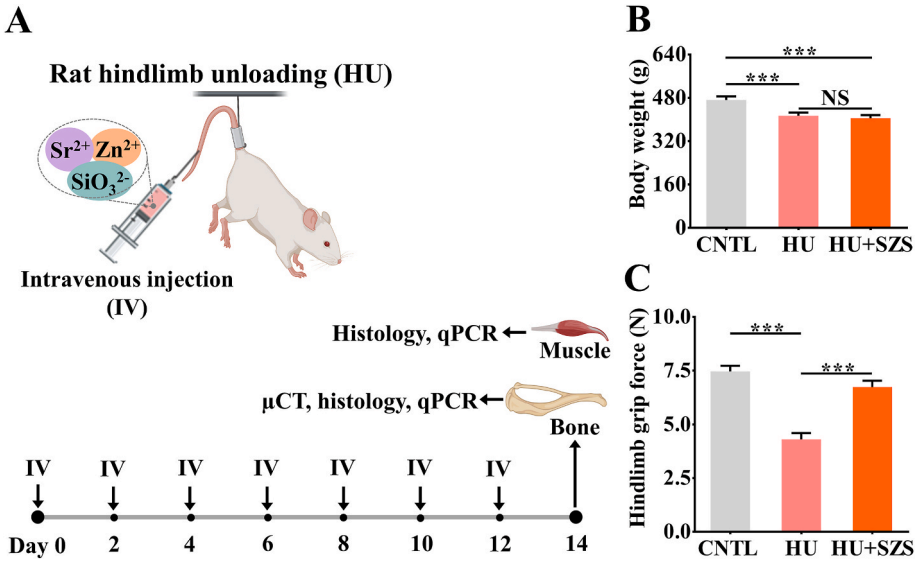

Figure 1. Schematic diagram of animal treatment with strontium zinc silicate (SZS) extract and the assessment of body weight and hindlimb grip force of rats. (**A**) Time schedule of hindlimb unloading (HU) and intravenous injection (IV) of SZS extract to rats. (**B**, **C**) Body weight (**B**) and hindlimb grip force (**C**) of rats at the end of the experiment. (n = 6) CNTL: age-matched control; HU: hindlimb unloading; HU + SZS: HU with SZS treatment.

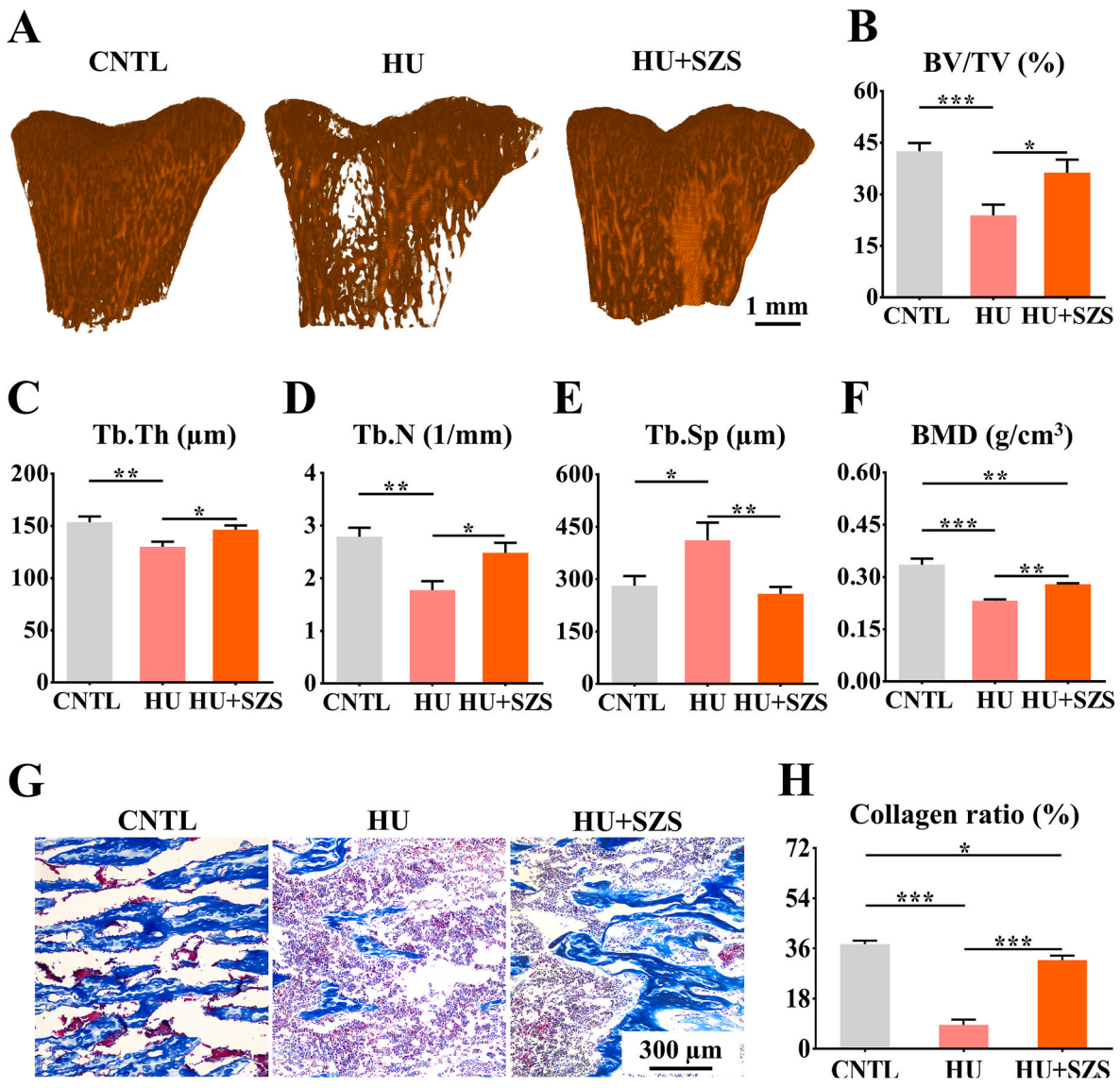

Figure 2. SZS extract prevents HU-induced microstructure deterioration and collagen reduction in rat tibias. (**A**) Representative 3D μCT images of the microstructure of trabecular bone in rat proximal tibias. (**B–F**) The quantitative statistics of bone volume fraction (BV/TV) (**B**), trabecular thickness (Tb.Th) (**C**), trabecular number (Tb.N) (**D**), trabecular separation (Tb.Sp) (**E**) and bone mineral density (BMD) (**F**) of the trabecular bone in proximal tibias from μCT analysis. (**G**) Representative images of Masson's trichrome staining of bone sections. (**H**) The quantitative evaluation of collagen ratio. (n = 6).

of CSA >4500 μm^2 were observed in the GA muscles of the HU rats compared to the CNTL rats, and these differences disappeared after SZS treatment of HU rats (Fig. 3G). Besides, a higher relative distribution of CSA <800 μm^2 and 800–1600 μm^2, together with a lower relative distribution of CSA >2400 μm^2 of the SOL muscles were found in the HU rats than in the CNTL rats (Fig. 3H). With SZS administration, only the relative distribution of SOL muscle fiber CSA <800 μm^2 in the HU + SZS group was significantly decreased when compared to the HU group. Thus, SZS treatment prohibited HU-induced muscle atrophy probably *via* dilating both small and large muscle fibers in the GA muscles, but only *via* dilating small muscle fibers in the SOL muscles. Together with muscle atrophy, more collagen formation was also observed in the GA and SOL muscles of HU rats compared to the CNTL rats (Fig. 3I–K). SZS treatment significantly reduced the collagen formation in the GA and SOL muscles of the HU rats, and the collagens in the GA and SOL muscles of the HU rats was almost completely and only partially recovered to the levels of the CNTL rats after SZS treatment, respectively (Fig. 3I–K). Collectively, SZS demonstrates effective inhibition of HU-induced skeletal muscle atrophy.

3.5. The underlying mechanisms of SZS extract prohibiting HU-induced osteosarcopenia

To explore the underlying mechanism of SZS extract-inhibited osteoporosis and sarcopenia in HU rats, the expression of mechanics-related, osteogenic and myogenic genes was analyzed. The relative mRNA expression of Piezo1 in the tibias and GA muscles was lower in the HU group than in the CNTL group (Fig. 4A). SZS treatment significantly increased the relative mRNA expression of Piezo1 in the tibias and GA muscles of the HU rats (Fig. 4A). Moreover, compared to the CNTL rats, HU rats had lower mRNA expression of Runx2 and higher mRNA expression of Col1α1 in the tibias, and SZS treatment significantly upregulated the relative mRNA expression of Runx2 and downregulated the relative mRNA expression of Col1α1 in the tibias of the HU rats (Fig. 4B and **C**). Other than in the bones, the relative mRNA expression of Myog and Mymk was upregulated and downregulated in the HU group compared to the CNTL group, respectively (Fig. 4D and **E**). With SZS management, the relative mRNA expression of Myog and Mymk in the GA muscles in HU rats was significantly increased to much higher

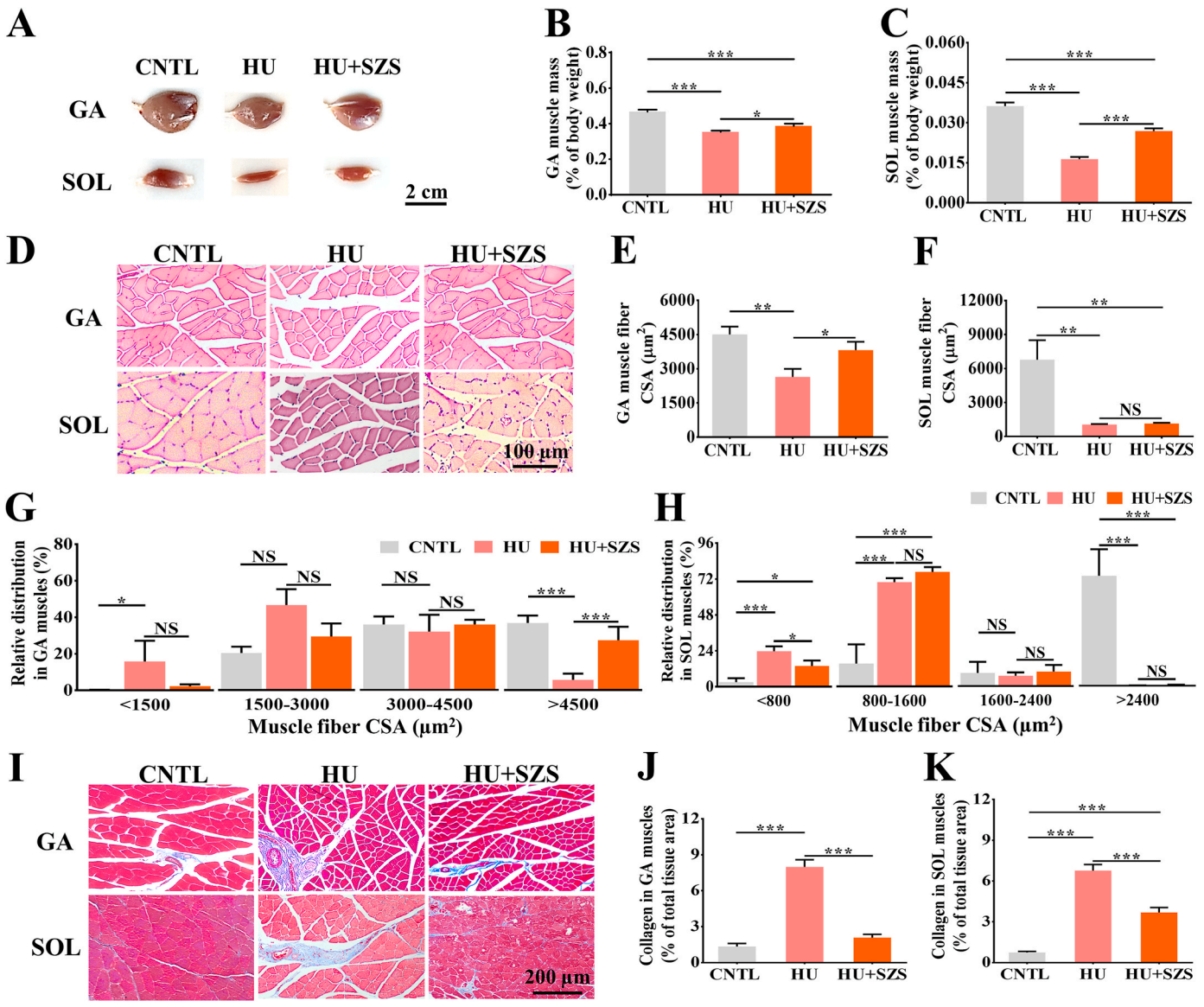

Figure 3. SZS extract prevents HU-induced atrophy and fibrosis in the gastrocnemius (GA) and soleus (SOL) muscles of rats. (**A**) Representative morphological diagram of the GA and SOL muscles. (**B**, **C**) The relative mass of GA (**B**) and SOL (**C**) muscles. (**D**) Representative images of H&E stained GA and SOL muscles. (**E**, **F**) The mean CSA of GA (**E**) and SOL (**F**) muscle fibers. (**G**, **H**) The relative distribution of the CSA of GA (**G**) and SOL (**H**) muscle fibers. (**I**) Representative images of the Masson's trichrome stained GA and SOL muscles. (**J**, **K**) The quantitative analysis of collagens in the GA (**J**) and SOL (**K**) muscles. (n = 6).

than the HU and CNTL groups (Fig. 4D and **E**). We speculated that SZS extract could enhance osteogenesis and myogenesis in the tibias and GA muscles *via* the Piezo1-mediated signaling.

To further validate the role of Piezo1 in SZS extract promoting osteogenesis and myogenesis, MC3T3-E1 and C2C12 cells were cultured, respectively. With 1/8 SZS extract and 1/128 SZS extract, vigorously enhanced cell viability was observed in the MC3T3-E1 and C2C12 cells, respectively (Figs. S4A and B). Based on the concentration of these SZS extracts, further *in vitro* study was conducted to examine their effect on Piezo1-mediated intracellular Ca^{2+}, and thus osteogenesis and myogenesis. GsMTx4 (Piezo1 inhibitor) downregulated the relative mRNA expression of Piezo1 while SZS extract upregulated the relative mRNA expression of Piezo1 by the MC3T3-E1 cells, and the SZS-induced upregulated Piezo1 gene expression was disappeared after Piezo1 blockage (Fig. 5A). Immunofluorescence staining results showed that GsMTx4 and SZS caused significantly lower and higher intracellular Ca^{2+} of the MC3T3-E1 cells than the CNTL group, respectively (Fig. 5B; Fig. S5A). After the inhibition of Piezo1 with GsMTx4, SZS treatment could not increase intracellular Ca^{2+} of the MC3T3-E1 cells (Fig. 5B; Fig. S5A). During the differentiation induction, upregulated gene expression of Runx2 and Col1α1 and more bone nodule formation were observed in the MC3T3-E1 cells cultured with SZS extract compared to those without (Fig. 5C and **D**; Fig. S5B). Similarly, the C2C12 cells treated with GsMTx4 and SZS exhibited significantly lower and higher mRNA expression of Piezo1 and intracellur Ca^{2+} than regular culture, respectively (Fig. 5E and **F**; Fig. S6A). The SZS-induced overexpression of Piezo1 mRNA and increase of intracellular Ca^{2+} were disappeared after Piezo1 blockage (Fig. 5E and **F**; Fig. S6A). Besides, higher expression of Myog and Mymk and more myotube formation were found in the C2C12 cells cultured with SZS extract than those without (Fig. 5G and **H**; Figs. S6B and C). Hence, SZS extract probably promoted Piezo1-regulated Ca^{2+} influx into osteoblasts and myoblasts, which contributes to osteogenesis and myogenesis.

4. Discussion

The maintenance of bone and muscle homeostasis depends on their adaptation to mechanical loading [5,6]. Physical inactivity usually

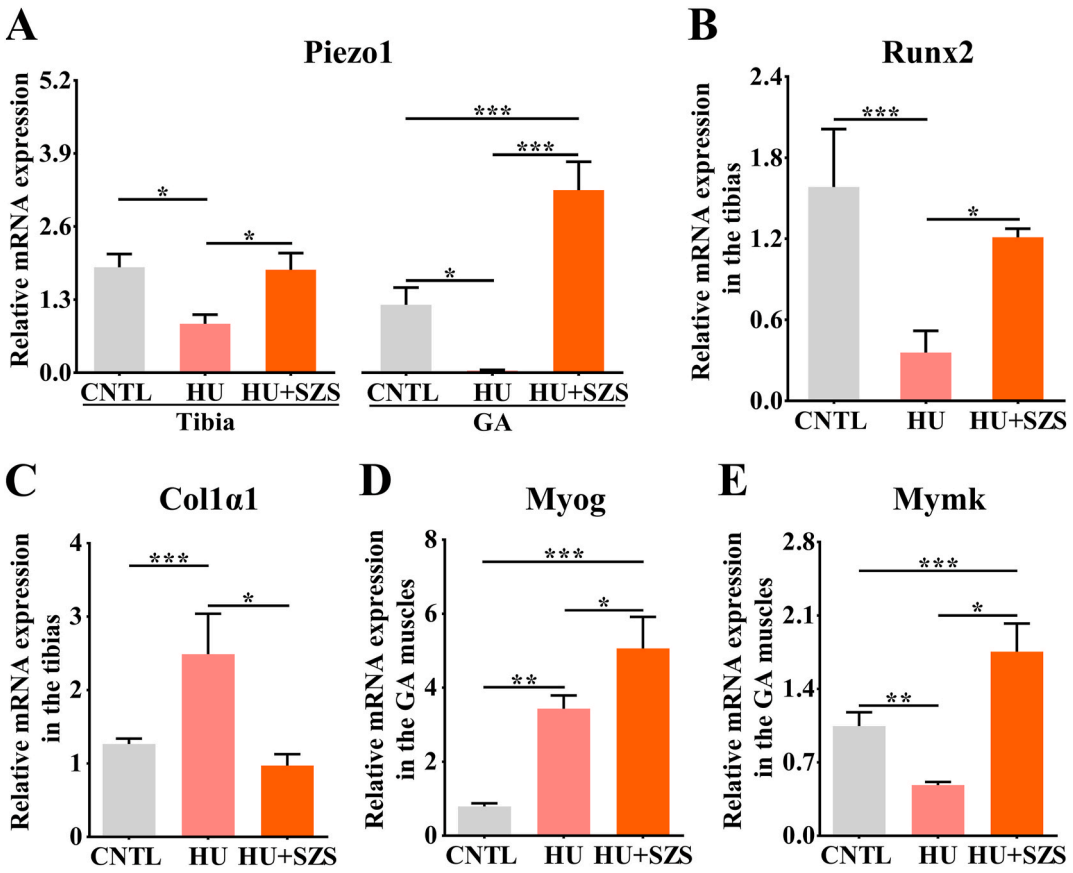

Figure 4. SZS extract prohibits HU-induced reduction in the mRNA expression of Piezo1 and osteogenic/myogenic factors in rat tibias and GA muscles. (**A**) The relative mRNA expression of Piezo1 in the tibias and GA muscles. (n = 5 for the CNTL group of tibias; n = 6 for the other groups) (**B**, **C**) The relative mRNA expression of Runx2 (**B**) and Col1α1 (**C**) in the tibias. (n = 6) (**D**, **E**) The relative mRNA expression of Myog (**D**) and Mymk (**E**) in the GA muscles. (n = 6).

elevates the probability of osteoporosis and sarcopenia, seriously affecting the life quality of people who suffer [1–3,29]. Mechanical stimulations such as physical exercise are commonly employed to counteract the disuse-induced osteoporosis and muscle waste [4,25,30]. However, they are not applicable for all patients. In this work, we developed a novel approach based on SZS biomaterials and validated the therapeutic efficacy of the SZS extract on HU-induced osteoporosis and muscle atrophy.

The idea was inspired by recent studies as biomaterials are garnering increasing interest in tissue regeneration because they have good biocompatibility and fewer side effects compared to pharmacological interventions [31]. One commonly applied strategy is to utilize the active components released from material degradation for different biological applications. In our study, after the treatment with SZS extract, we got even more efficient restoration of the deteriorated bones and atrophic muscles in the HU rats compared to the traditional mechanical stimulations reported in other studies [32,33]. SZS treatment restored the relative mass of SOL muscles in the HU rats from 45.03 % to 74.25 % of the CNTL rats in our study, while climbing exercise has little effect on the recovery of the HU-induced decrease of SOL muscle wet weight [32]. Also, eight weeks' vibrations and resistance exercise can reinstate the halved relative SOL muscle mass in HU rats to approximately 60 % of the CNLT rats [34], while in our study, administration with SZS extract rehabilitated the halved relative SOL muscle mass in HU rats to 74.25 % of the CNTL rats. In the aspect of bone recovery, our SZS extract exhibited a comparable effect on the prohibition of HU-induced bone loss compared to the vibration and resistance exercise [34]. However, our intervention period is much shorter than the vibration and resistance exercise. In addition, our study showed faster recovery of the reduced bone volume fraction in the proximal tibias of HU rats (restored to 85.35 % of the CNTL group), when compared to another study where electrical stimulation is utilized to prevent HU-induced bone loss (restored to 65.63 % of the CNTL group) [33]. Therefore, SZS extract presents comparable or higher efficacy in prohibiting HU-induced osteoporosis and sarcopenia compared to conventional mechanical stimulations or other alternative methods.

The SZS extract enhanced recovery of atrophic muscle and osteoporotic bone in HU rats is probably attributed to the combination of Zn^{2+}, Sr^{2+} and SiO_3^{2-}. Sr, Zn and Si exhibit regenerative potential for both bone and muscle, respectively [24,35–40]. However, a single element Sr, Zn or Si is considered to have limited therapeutic effects, while ion combination may have synergistic activity in stimulating tissue regeneration. For example, the combination of Sr^{2+} and SiO_3^{2-} has been proven to have synergistic effects on the regeneration of osteoporotic bone [21]. This is attributed to the dominant effects of Sr^{2+} on enhancing angiogenesis and repressing osteoclastogenesis, and the dominant effects of SiO_3^{2-} on stimulating osteogenesis. In another case, the combination of Zn^{2+} and SiO_3^{2-} demonstrated enhanced intracellular reactive oxygen species (ROS) scavenging efficacy and anti-cardiomyocyte apoptosis ability compared to single SiO_3^{2-} [40]. This was due to the superior mitochondrial preservation provided by Zn^{2+}, resulting in better therapeutic effects for ischemic myocardial disease. In current work, our *in vitro* study showed that SZS extract increased the Piezo1 gene expression and intracellular Ca^{2+} in the MC3T3-E1 cells and C2C12 cells, which was almost totally blocked after inhibiting Piezo1. This suggests that the combination of Zn^{2+}, Sr^{2+} and SiO_3^{2-} probably increases intracellular Ca^{2+} mainly through the Piezo1 channel in osteoblasts and myoblasts. The increase of intracellular Ca^{2+} may promote the activation of Akt and further stimulate osteogenic differentiation of bone marrow mesenchymal stem cells and protein

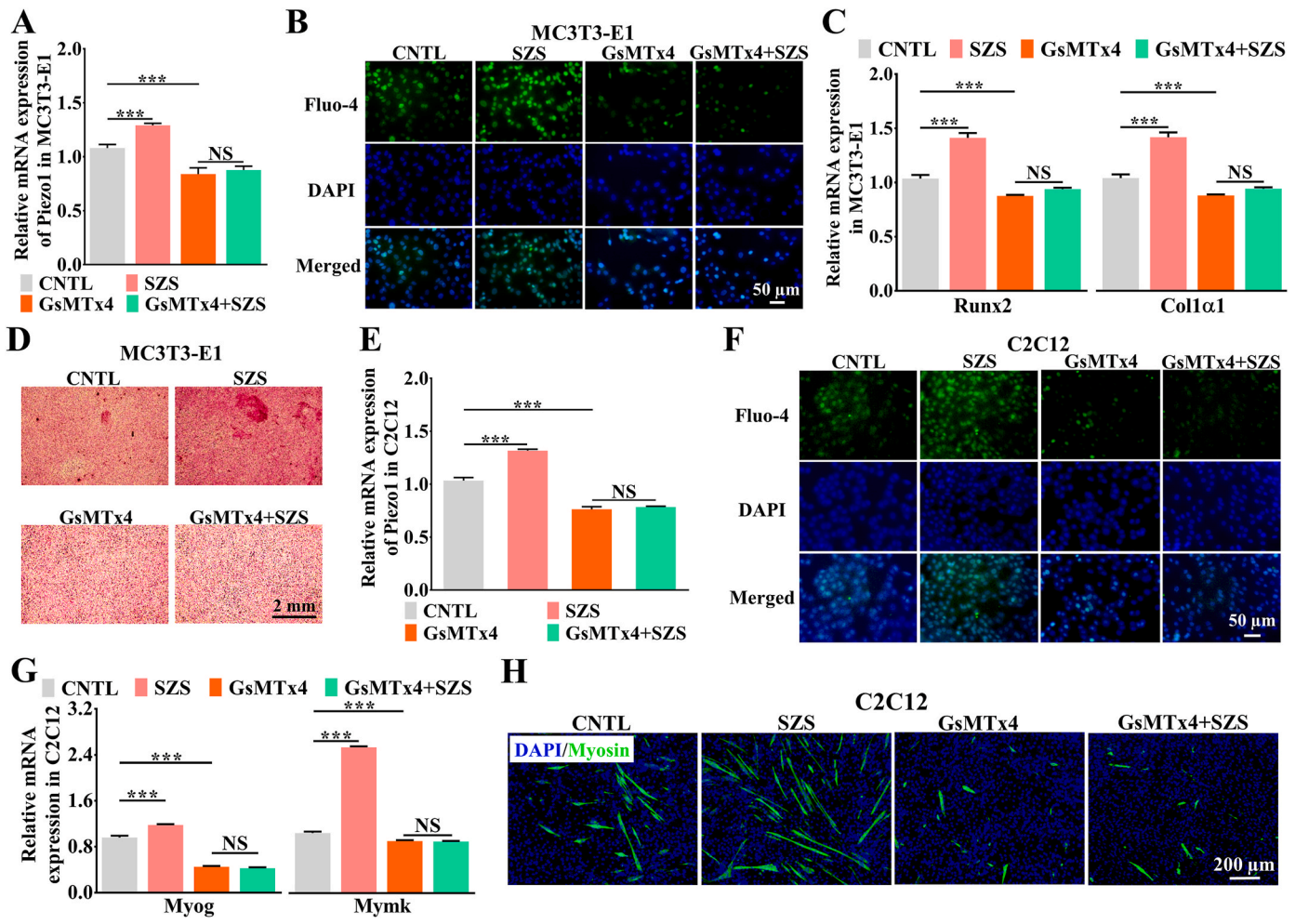

Figure 5. SZS extract increases Piezo1-mediated intracellular Ca^{2+} and thus promotes osteogenic differentiation of MC3T3-E1 cell and myogenic differentiation of C2C12 cells. (**A**) The relative mRNA expression of Piezo1 by MC3T3-E1 cells cultured with or without SZS extract or 0.5 μM GsMTx4 (Piezo1 inhibitor) for 48 h. (**B**) Representative immunofluorescence images of intracellular Ca^{2+} (loaded with 5 μM Fluo-4) of MC3T3-E1 cells cultured with or without SZS extract or 0.5 μM GsMTx4 for 48 h. (**C**) The relative mRNA expression of Runx2 and Col1α1 by MC3T3-E1 cells cultured with or without SZS extract or 0.5 μM GsMTx4 for 48 h. (**D**) Representative alizarin red S stained images of MC3T3-E1 cells cultured in differentiation medium for one week. (**E**) The relative mRNA expression of Piezo1 by C2C12 cells cultured with or without SZS extract or 0.5 μM GsMTx4 for 48 h. (**F**) Representative immunofluorescence images of intracellular Ca^{2+} (loaded with 5 μM Fluo-4) of C2C12 cells cultured with or without SZS extract or 0.5 μM GsMTx4 for 48 h. (**G**) The relative mRNA expression of Myog and Mymk by C2C12 cells cultured with or without SZS extract or 0.5 μM GsMTx4 for 48 h. (**H**) Representative immunofluorescence images of myotubes of C2C12 cells cultured in differentiation medium with or without SZS extract or 0.5 μM GsMTx4 for five days. (n = 6). (For interpretation of the references to color in this figure legend, the reader is referred to the Web version of this article.)

synthesis in skeletal muscle cells [9–11]. Previous studies have also revealed that the activation of Akt-related signaling pathways not only regulates osteoblastic differentiation and the production of alkaline phosphatase to form bone matrix, but also affects the expression of myogenic differentiation factor Myog and myoblast fusion factor Mymk and the protein synthesis to maintain muscle homeostasis [9–11,41]. Furthermore, intracellular Ca^{2+} also contributes to muscle contraction, the regulation of myocyte-to-myotube fusion and the insulin-like growth factor 1 (IGF-1)-induced osteogenic differentiation in bone marrow mesenchymal stem cells, together with the upregulation of osteogenic markers Runx2, Col1α1 and bone morphogenetic proteins by osteoblasts [10,42,43]. Therefore, SZS extract is probably able to replicate the effect of mechanical loading to counteract the HU-induced osteoporosis and sarcopenia concurrently by the enhancement of osteogenesis and myogenesis simultaneously *via* promoting Piezo1-mediated intracellular Ca^{2+} in osteoblasts and myoblasts (Fig. 6).

It's worth mentioning that HU can lead to excessive collagen deposition in skeletal muscles [44]. The excessive deposition of extracellular matrix results in fibrosis, which hampers the migration of satellite cells and thus hinders muscle fiber dilation [45]. In this work, we demonstrated that SZS treatment could inhibit HU-induced fibrosis in both GA and SOL muscles. The combination of Zn^{2+}, Sr^{2+} and SiO_3^{2-} ions may play a major role, as each element exhibited anti-fibrosis potential in other tissues [46–48]. Their specific cellular regulation capacities, such as regulating immune cells to inhibit inflammatory factor secretion and stimulating tissue cells to regenerate, contribute to forming healthy tissues and preventing fibrosis [46–48]. In addition, our results demostarted that SZS extract prohibited HU-induced atrophy differently in the GA and SOL muscles. SZS treatment significantly increased the volume and relative mass of both GA and SOL muscles, but only increased the mean CSA of GA muscles of the HU rats. It seems SZS administration obstructed the growth of muscle fibers in the SOL muscles compared with GA muscles. In our work, SZS treatment only partially recovered the HU-induced SOL muscle fibrosis, while SZS treatment nearly totally restored the HU-induced GA muscle fibrosis. Therefore, severe muscle fibrosis may be the reason that SZS treatment had a weaker effect on the regeneration of SOL muscles than GA muscles. Combined with the fact that GA muscles contain fast- and

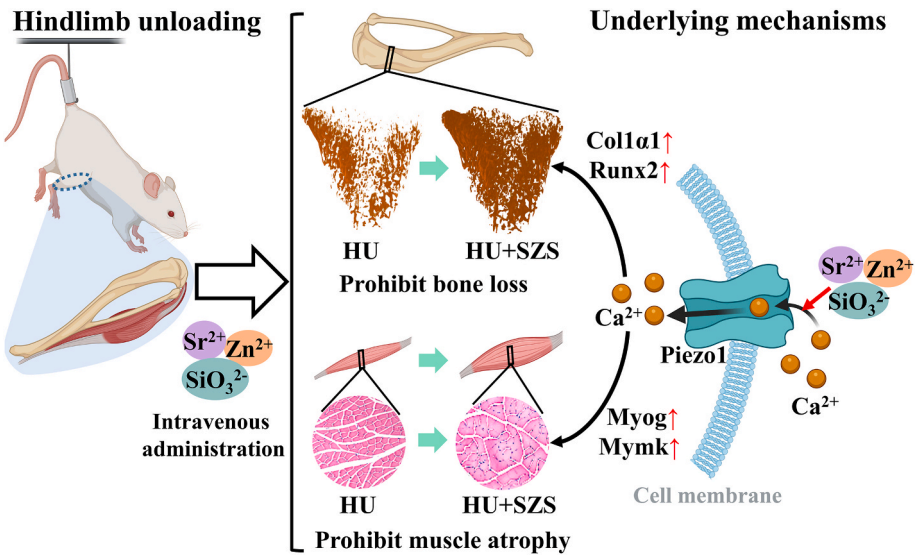

Figure 6. Schematic diagram of SZS extract concurrently prohibiting HU-induced bone loss and muscle atrophy. The Sr^{2+}, Zn^{2+} and SiO_3^{2-} in SZS extract promotes Piezo1-mediated Ca^{2+} influx which contributes to the upregulation of Runx2 and Col1α1 in bones and Myog and Mymk in muscles. As a consequence, the HU-induced bone structural deterioration, muscle volume reduction and muscle fiber atrophy is prohibited.

slow-twitch muscle fibers and SOL muscles contain mainly slow-twitch muscle fibers [49,50], we speculate that the slow-twitch muscle fibers delayed the SOL muscle recovery from fibrosis after SZS treatment. As a consequence, the retained fibrosis in the slow-twitch muscle fibers probably impedes the SZS-induced muscle regeneration in the HU rats. Thus, the elimination of muscle fibrosis is probably a prerequisite for efficient muscle regeneration.

In conclusion, SZS extract can simultaneously prohibit HU-induced osteopenia and sarcopenia, implying the ability of SZS extract to replicate the effect of mechanical stimulation on both bone and muscle. The Sr^{2+}, Zn^{2+} and SiO_3^{2-} released from SZS increase the intracellular Ca^{2+} of osteoblasts and myoblasts *via* the Piezo1 ion channel to improve osteogenesis and myogenesis. This study may provide a new avenue to a universally applicable, efficient, and concurrent intervention of osteoporosis and sarcopenia. The preliminary clarification of underlying biological mechanisms establishs a theoretical foundation for the application of bioactive ceramics in regenerative medicine.

Author contributions

LH, YJ, CY and JC formulated the hypothesis and designed the experiments. LH performed the main work of achieving experiments, analyzing data and drafting the manuscript. HX and HL Formal analysis. JY and CW prepared and characterized the SZS powders and extracts. YQ performed the collection of bone and muscle samples. ZZ, YJ and CF optimized the procedure of histological sample preparation of muscles. LH, YJ, CY and JC contributed to the revision of the manuscript.

Data availability statement

The data generated in this study are available from the corresponding author upon reasonable request.

Declaration of AI and AI-assisted technologies in the writing process

The authors delare no AI-assisted technologies in the writing process.

Acknowledgments

The authors would like to acknowledge the support of the National Key Research and Development Program of China (2023YFB3810202), the National Natural Science Foundation of China (32271386), the Opening Research fund from Shanghai Key Laboratory of Stomatology, Shanghai Ninth People's Hospital, College of Stomatology, Shanghai Jiao Tong University School of Medicine (Grant No. 2022SKLS-KFKT005), the Wenzhou Basic Scientific Research Project (Y2023068), the seed grants from the Wenzhou Institute, University of Chinese Academy of Sciences (WIUCASQD2020013, WIUCASQD2021030, WIUCASQD2021029, WIUCASQD2022032, WIUCASQD2023019), and the funding from the First Affiliated Hospital of Wenzhou Medical University.

Appendix A. Supplementary data

Supplementary data to this article can be found online at https://doi.org/10.1016/j.jot.2024.07.014.

All persons who meet authorship criteria are listed as authors, and all authors certify that they have participated sufficiently in the work to take public responsibility for the content, including participation in the concept, design, analysis, writing, or revision of the manuscript. Each author certifies that this material or part thereof has not been published in another journal, that it is not currently submitted elsewhere, and that it will not be submitted elsewhere until a final decision regarding publication of the manuscript in Journal of Orthopaedic Translation has been made.

The corresponding author agrees to pay the Journal of Orthopaedic Translation Article Processing Charge upon acceptance of the work for publication in Journal of Orthopaedic Translation, unless prior arrangements have been made to waive the Article Processing Charge.

References

[1] Leone GE, Shields DC, Haque A, Banik NL. Rehabilitation: neurogenic bone loss after spinal cord injury. Biomedicines 2023;11(9):2581.
[2] Kirk B, Miller S, Zanker J, Duque G. A clinical guide to the pathophysiology, diagnosis and treatment of osteosarcopenia. Maturitas 2020;140:27–33.
[3] Stein TP. Weight, muscle and bone loss during space flight: another perspective. Eur J Appl Physiol 2013;113(9):2171–81.
[4] Papadopoulou SK, Papadimitriou K, Voulgaridou G, Georgaki E, Tsotidou E, Zantidou O, et al. Exercise and nutrition impact on osteoporosis and sarcopenia-the incidence of osteosarcopenia: a narrative review. Nutrients 2021;13(12):4499.
[5] Wang L, You X, Zhang L, Zhang C, Zou W. Mechanical regulation of bone remodeling. Bone Res 2022;10(1):16.

[6] Graham ZA, Lavin KM, O'Bryan SM, Thalacker-Mercer AE, Buford TW, Ford KM, et al. Mechanisms of exercise as a preventative measure to muscle wasting. Am J Physiol Cell Physiol 2021;321(1):C40–57.
[7] Dienes B, Bazso T, Szabo L, Csernoch L. The role of the Piezo1 mechanosensitive channel in the musculoskeletal system. Int J Mol Sci 2023;24(7):6513.
[8] Kefauver JM, Ward AB, Patapoutian A. Discoveries in structure and physiology of mechanically activated ion channels. Nature 2020;587(7835):567–76.
[9] Danciu TE, Adam RM, Naruse K, Freeman MR, Hauschka PV. Calcium regulates the PI3K-Akt pathway in stretched osteoblasts. FEBS Lett 2003;536(1–3):193–7.
[10] Wu L, Zhang G, Guo C, Pan Y. Intracellular Ca(2+) signaling mediates IGF-1-induced osteogenic differentiation in bone marrow mesenchymal stem cells. Biochem Biophys Res Commun 2020;527(1):200–6.
[11] Gorelick-Feldman J, Cohick W, Raskin I. Ecdysteroids elicit a rapid Ca2+ flux leading to Akt activation and increased protein synthesis in skeletal muscle cells. Steroids 2010;75(10):632–7.
[12] Wang J, Sun YX, Li J. The role of mechanosensor Piezo1 in bone homeostasis and mechanobiology. Dev Biol 2023;493:80–8.
[13] Li X, Han L, Nookaew I, Mannen E, Silva MJ, Almeida M, et al. Stimulation of Piezo1 by mechanical signals promotes bone anabolism. Elife 2019;8:e49631.
[14] Peng Y, Du J, Gunther S, Guo X, Wang S, Schneider A, et al. Mechano-signaling via Piezo1 prevents activation and p53-mediated senescence of muscle stem cells. Redox Biol 2022;52:102309.
[15] Hirata Y, Nomura K, Kato D, Tachibana Y, Niikura T, Uchiyama K, et al. A Piezo1/KLF15/IL-6 axis mediates immobilization-induced muscle atrophy. J Clin Invest 2022;132(10):1–13.
[16] Hess P, Tsien RW. Mechanism of ion permeation through calcium channels. Nature 1984;309(5967):453–6.
[17] Gottlieb PA, Sachs F. Piezo1: properties of a cation selective mechanical channel. Channels 2012;6(4):214–9.
[18] Najda J, Gminski J, Drozdz M, Danch A. The action of excessive, inorganic silicon (Si) on the mineral metabolism of calcium (Ca) and magnesium (Mg). Biol Trace Elem Res 1993;37(2–3):107–14.
[19] Shie MY, Ding SJ, Chang HC. The role of silicon in osteoblast-like cell proliferation and apoptosis. Acta Biomater 2011;7(6):2604–14.
[20] Valerio P, Pereira MM, Goes AM, Leite MF. BG60S dissolution interferes with osteoblast calcium signals. J Mater Sci Mater Med 2007;18(2):265–71.
[21] Mao L, Xia L, Chang J, Liu J, Jiang L, Wu C, et al. The synergistic effects of Sr and Si bioactive ions on osteogenesis, osteoclastogenesis and angiogenesis for osteoporotic bone regeneration. Acta Biomater 2017;61:217–32.
[22] Lin YH, Lee AK, Ho CC, Fang MJ, Kuo TY, Shie MY. The effects of a 3D-printed magnesium-/strontium-doped calcium silicate scaffold on regulation of bone regeneration via dual-stimulation of the Akt and Wnt signaling pathways. Biomater Adv 2022;133:112660.
[23] Yu J, Xu Y, Zhang Z, Zeng Z, Chen D, Wei Z, et al. Strontium zinc silicate bioceramic composite electrospun fiber membrane for hair follicle regeneration in burn wounds. Compos B Eng 2023;266:110953.
[24] Pan H, Deng L, Huang L, Zhang Q, Yu J, Huang Y, et al. 3D-printed Sr(2)ZnSi(2)O(7) scaffold facilitates vascularized bone regeneration through macrophage immunomodulation. Front Bioeng Biotechnol 2022;10:1007535.
[25] Yang PF, Huang LW, Nie XT, Yang Y, Wang Z, Ren L, et al. Moderate tibia axial loading promotes discordant response of bone composition parameters and mechanical properties in a hindlimb unloading rat model. J Musculoskelet Neuronal Interact 2018;18(2):152–64.
[26] Apseloff G, Girten B, Walker M, Shepard DR, Krecic ME, Stern LS, et al. Aminohydroxybutane bisphosphonate and clenbuterol prevent bone changes and retard muscle atrophy respectively in tail-suspended rats. J Pharmacol Exp Therapeut 1993;264(3):1071–8.
[27] Livak KJ, Schmittgen TD. Analysis of relative gene expression data using real-time quantitative PCR and the 2(-Delta Delta C(T)) Method. Methods 2001;25(4):402–8.
[28] Qin L, He T, Chen S, Yang D, Yi W, Cao H, et al. Roles of mechanosensitive channel Piezo1/2 proteins in skeleton and other tissues. Bone Res 2021;9(1):44.
[29] Konda NN, Karri RS, Winnard A, Nasser M, Evetts S, Boudreau E, et al. A comparison of exercise interventions from bed rest studies for the prevention of musculoskeletal loss. NPJ microgravity 2019;5:12.
[30] Atkins KD, Bickel CS. Effects of functional electrical stimulation on muscle health after spinal cord injury. Curr Opin Pharmacol 2021;60:226–31.
[31] Mbese Z, Aderibigbe BA. Bisphosphonate-based conjugates and derivatives as potential therapeutic agents in osteoporosis, bone cancer and metastatic bone cancer. Int J Mol Sci 2021;22(13):6869.
[32] Allen DL, Linderman JK, Roy RR, Grindeland RE, Mukku V, Edgerton VR. Growth hormone/IGF-I and/or resistive exercise maintains myonuclear number in hindlimb unweighted muscles. J Appl Physiol 1997;83(6):1857–61.
[33] Lau YC, Qian X, Po KT, Li LM, Guo X. Electrical stimulation at the dorsal root ganglion preserves trabecular bone mass and microarchitecture of the tibia in hindlimb-unloaded rats. Osteoporos Int 2015;26(2):481–8.
[34] Li Z, Tan C, Wu Y, Ding Y, Wang H, Chen W, et al. Whole-body vibration and resistance exercise prevent long-term hindlimb unloading-induced bone loss: independent and interactive effects. Eur J Appl Physiol 2012;112(11):3743–53.
[35] Yuan Y, Zhang Z, Mo F, Yang C, Jiao Y, Wang E, et al. A biomaterial-based therapy for lower limb ischemia using Sr/Si bioactive hydrogel that inhibits skeletal muscle necrosis and enhances angiogenesis. Bioact Mater 2023;26:264–78.
[36] Yu X, Gholipourmalekabadi M, Wang X, Yuan C, Lin K. Three-dimensional bioprinting biphasic multicellular living scaffold facilitates osteochondral defect regeneration. Interdiscip Mater 2024;3:1–19.
[37] Yu X, Jiang S, Li D, Shen SGF, Wang X, Lin K. Osteoimmunomodulatory bioinks for 3D bioprinting achieve complete regeneration of critical-sized bone defects. Compos B Eng 2024;273:111256.
[38] Zhuang Y, Liu A, Jiang S, Liaqat U, Lin K, Sun W, et al. Promoting vascularized bone regeneration via strontium-incorporated hydroxyapatite bioceramic. Mater Des 2023;234:112313.
[39] Gao J, Nie W, Xing K, Guo Y. Comparative study of different maternal zinc resource supplementation on performance and breast muscle development of their offspring. Biol Trace Elem Res 2019;190(1):197–207.
[40] Zhang Y, Li X, Zhang Z, Li H, Chen D, Jiao Y, et al. Zn(2)SiO(4) bioceramic attenuates cardiac remodeling after myocardial infarction. Adv Healthc Mater 2023;12(21):e2203365.
[41] Luo W, Lin Z, Chen J, Chen G, Zhang S, Liu M, et al. TMEM182 interacts with integrin beta 1 and regulates myoblast differentiation and muscle regeneration. J Cachexia Sarcopenia Muscle 2021;12(6):1704–23.
[42] Sinha S, Elbaz-Alon Y, Avinoam O. Ca(2+) as a coordinator of skeletal muscle differentiation, fusion and contraction. FEBS J 2022;289(21):6531–42.
[43] Kito H, Ohya S. Role of K(+) and Ca(2+)-permeable channels in osteoblast functions. Int J Mol Sci 2021;22(19):10459.
[44] Petrocelli JJ, McKenzie AI, de Hart N, Reidy PT, Mahmassani ZS, Keeble AR, et al. Disuse-induced muscle fibrosis, cellular senescence, and senescence-associated secretory phenotype in older adults are alleviated during re-ambulation with metformin pre-treatment. Aging Cell 2023;22(11):e13936.
[45] Mahdy MAA. Skeletal muscle fibrosis: an overview. Cell Tissue Res 2019;375(3):575–88.
[46] Xing M, Jiang Y, Bi W, Gao L, Zhou YL, Rao SL, et al. Strontium ions protect hearts against myocardial ischemia/reperfusion injury. Sci Adv 2021;7(3):eabe0726.
[47] Aksoy-Ozer ZB, Bitirim CV, Turan B, Akcali KC. The role of zinc on liver fibrosis by modulating ZIP14 expression throughout epigenetic regulatory mechanisms. Biol Trace Elem Res 2024:1–12.
[48] Chen T, Zhang Z, Weng D, Lu L, Wang X, Xing M, et al. Ion therapy of pulmonary fibrosis by inhalation of ionic solution derived from silicate bioceramics. Bioact Mater 2021;6(10):3194–206.
[49] Ishihara A, Taguchi S. Histochemical differentiation of fibers in the rat slow and fast twitch muscles. Jpn J Physiol 1991;41(2):251–8.
[50] Edgerton VR, Smith JL, Simpson DR. Muscle fibre type populations of human leg muscles. Histochem J 1975;7(3):259–66.